The Limb Adjustment of AMSU-A Observations: Methodology and Validation

MITCHELL D. GOLDBERG

National Oceanic and Atmospheric Administration, National Environmental Satellite, Data, and Information Service, Office of Research and Applications, Washington, D.C.

DAVID S. CROSBY

National Oceanic and Atmospheric Administration, National Environmental Satellite, Data, and Information Service, Office of Research and Applications, Washington, D.C., and American University, Washington, D.C.

LIHANG ZHOU

QSS Group Inc., Lanham, Maryland

(Manuscript received 3 January 2000, in final form 10 May 2000)

ABSTRACT

The Advanced Microwave Sounding Unit-A (AMSU-A) is the first of a new generation of polar-orbiting cross-track microwave sounders operated by the National Oceanic and Atmospheric Administration. A feature of a cross-track sounder is that the measurements vary with scan angle because of the change in the optical pathlength between the earth and the satellite. This feature is called the limb effect and can be as much as 30 K. One approach to this problem is to limb adjust the measurements to a fixed view angle. This approach was used for the older series of Microwave Sounding Units. Limb adjusting is important for climate applications and regression retrieval algorithms. This paper describes and evaluates several limb adjustment procedures. The recommended procedure uses a combined physical and statistical technique. The limb adjusted measurements were compared with computed radiances from radiosondes and National Centers for Environmental Prediction models. The model error was found to be less than the instrument noise for most of the temperature sounding channels. The error in the window channels was small relative to the observed range of these channels. Limb adjusted fields appear to be smooth. Statistical tests of the distributions of the adjusted measurements at each scan angle show them to be very similar.

1. Introduction

Replacing the older series of the Microwave Sounding Units (MSU) (Smith et al. 1979), the Advanced Microwave Sounding Unit-A (AMSU-A) is the first of a new generation of polar-orbiting cross-track microwave sounders operated by the National Ocean and Atmospheric Administration (NOAA). The first AMSU-A was launched on the *NOAA–15* satellite, 13 May 1998 and measures outgoing radiation from the earth's surface and/or atmosphere in 15 spectral regions (four ''window'' channels at 23.8, 31.4, 50.3, and 89 GHz and 11 temperature sounding channels from 52.8 to 58 GHz). We use the term window for channels having a surface contribution of 70% or more. The temperature sounding channels are used to derive atmospheric temperature profiles from the surface to an altitude of about 40 km in most situations. The exceptions are in regions of precipitation that can cause erroneous estimates of temperature in the lower troposphere (Goldberg 1999). The window channels receive energy primarily from the surface and the boundary layer, and are used in deriving total precipitable water, cloud liquid water, snow cover, sea ice concentration, and precipitation rate (Grody et al. 1999).

A feature of a cross-track sounder is the variation of the measurement along the scan line. This variation is caused by the change in the optical path length between the earth and the satellite. The AMSU-A scans between $\pm 48.3333°$ off nadir with 30 beam positions per scan line and a swath width of about 2300 km. The variation of the measurement as a function of beam position is called the limb effect and can be as much as 30 K for the 23.8-GHz window channel and 15 K for the atmospheric temperature channels (53–58 GHz). Limb adjusting the measurement to a fixed view angle is a common practice at NOAA (Wark 1993) and is important

Corresponding author address: Mitchell D. Goldberg, NOAA/NESDIS, 5200 Auth Road, Rm. 810, Camp Springs, MD 20746.
E-mail: mgoldberg@nesdis.noaa.gov

TABLE 1. Instrument characteristics of the AMSU-A.

Channel number	Channel frequency (MHz)	No. bands	Measured RF 3-db bandwidth (MHz)	NEDT (K)	
				Spec.	Measured
1	23 800	1	251.02	0.30	0.211
2	31 400	1	161.20	0.30	0.265
3	50 300	1	161.14	0.40	0.219
4	52 800	1	380.52	0.25	0.143
5	53 596 ± 115	2	168.20	0.25	0.148
6	54 400	1	380.54	0.25	0.154
7	54 940	1	380.56	0.25	0.132
8	55 500	1	310.34	0.25	0.141
9	f_0 = 57 290.344	1	310.42	0.25	0.236
10	f_0 ± 217	2	76.58	0.40	0.250
11	f_0 ± 322.2 ± 48	4	35.11	0.40	0.280
12	f_0 ± 322.2 ± 22	4	15.29	0.60	0.399
13	f_0 ± 322.2 ± 10	4	7.93	0.80	0.539
14	f_0 ± 322.2 ± 4.5	4	2.94	1.20	0.914
15	89 000	1	1998.98	0.50	0.165

for a number of applications. Regression algorithms that depend on collocated observations of satellite data and in situ data, such as radiosonde reports of temperature, to derive the statistical relationship (i.e., equation) to estimate geophysical parameters, such as atmospheric temperatures, from satellite observations are simplified if the satellite data are normalized to a fixed angle. Otherwise there would be difficulty in achieving a reasonable sample size for each beam position. Regression retrievals, derived from satellite observations that are not adjusted to a common view angle, will probably suffer from spot-to-spot systematic errors if the temporal distribution and sample size of the collocated data, as a function of beam position vary considerably. [In this paper, beam position, field-of-view (FOV), and spot are synonymous.] Physical retrieval algorithms often retrieve along the optical path, but generally some sort of beam position-dependent bias adjustment is needed to remove spot-to-spot systematic biases caused by asymmetry of the observations (discussed further in the next section). If the limb adjustment procedure produced accurate limb adjusted data, then a physical retrieval would be simplified since there would be no need for spot-dependent bias adjustments. Last, averaging satellite observations to a given grid map (e.g., monthly $1^\circ \times 1^\circ$ latitude/longitude, zonal bands) requires that the data are limb adjusted prior to averaging. Otherwise the data averaged will be associated with different atmospheric weighting functions. Observations representative of a fixed weighting function are critical for climate monitoring (Goldberg and Fleming 1995).

The purpose of this paper is to describe and verify our limb adjustment procedure for AMSU-A. Our limb adjusted AMSU-A observations have been used in deriving daily temperature time series at various levels in the troposphere and stratosphere (Goldberg 1999) and to estimate the strength of tropical storms (Kidder et al. 2000).

2. AMSU-A observations and limb adjustment

The AMSU-A consists of two separate modules, A1 and A2. The A1 component has 12 channels between 50 and 58 GHz in the oxygen band and an 89-GHz window channel. Even though channel 4, 50.3 GHz, is in the oxygen band, we refer to it as a window channel since most of the energy measured for this channel is from the surface. The A2 has two window channels at 23.8 and 31.4 GHz. Note that channel 1, 23.8 GHz, is located at a weak water vapor line. There are 30 measurements per scan line; positions 15 and 16 have near-nadir angles of 1.67°, while positions 1 and 30 are at the extreme scan positions. The FOV size is 48 km in diameter at the near-nadir positions and grows gradually to about 150 km at positions 1 and 30. The AMSU-A instrument parameters are provided in Table 1.

Prior to limb adjustment a correction is made for antenna side lobes. At each scan position, the main antenna lobe points at the earth, but side lobes can point at different points on the earth, at cold space, and at the spacecraft itself. The raw measurements, called antenna temperatures, are converted to brightness temperatures using an algorithm developed by Mo (1999), which removes the contribution from the instrument and space by accounting for the instrument's antenna pattern. We tested the antenna correction procedure for channels 4–14 as a function of FOV by comparing the bias between observed antenna temperatures and computed brightness temperatures, using the OPTRAN radiative transfer code (McMillin et al. 1995) with state parameters obtained from the National Centers for Environmental Prediction (NCEP) analysis of atmospheric temperature, surface temperature, and water vapor, with the bias between brightness temperatures computed using Mo's algorithm, and the same computed NCEP brightness temperatures (see Fig. 1). The NCEP analysis used was from ocean regions and did not include information from AMSU-A. The ocean surface emissivity compu-

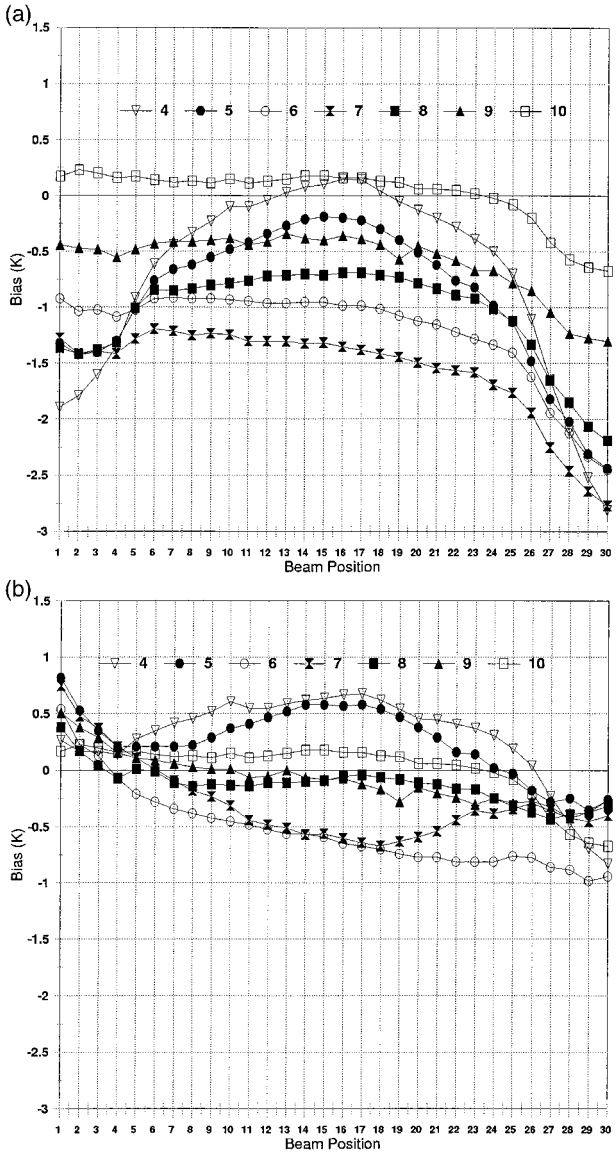

FIG. 1. (a) The mean bias of the difference between AMSU-A antenna temperatures and brightness temperatures computed from an NCEP analysis, and (b) the mean bias of the difference between AMSU-A brightness temperatures and the brightness temperatures computed from an NCEP analysis.

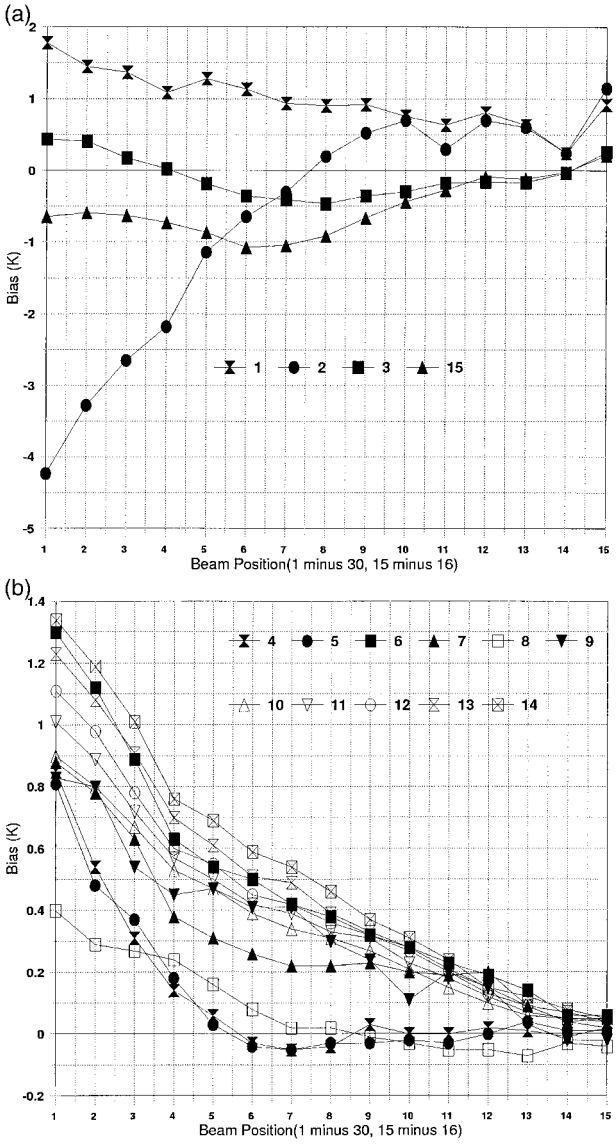

FIG. 2. The mean bias (i.e., asymmetry) between unadjusted brightness temperatures from field-of-views with the same off-nadir angles: (a) the bias from the window channels; (b) the bias from the atmospheric channels.

tation, needed for the forward calculation of brightness temperatures, is based on Klein and Swift (1977) for calm water and modified to account for surface wind speed using the rough sea model developed by Hollinger (1971). As shown in Fig. 1, there is better agreement between the measured and computed values after the conversion of antenna temperature to brightness temperature. However, the bias is not zero, nor even constant with FOV position, which is expected if there were no errors in the antenna patterns and the radiative transfer equation. Figure 2 illustrates the asymmetry present in AMSU-A brightness temperatures. Plotted in this figure is the difference between beam positions with the same off-nadir angle, that is, the mean difference of measurements from FOV 30 and FOV 1 to FOV 16 and FOV 15. The means were computed from data collected over oceanic regions between $\pm 60^\circ$ latitude and for the time period of 1–5 May 1999. A 5-day period is used to minimize FOV-dependent horizontal variability of the surface and atmosphere. All figures presented in this paper, unless otherwise noted, are derived from this time period. If there were no asymmetry the difference should be zero for each pair. Note that because the antenna correction is nearly symmetrical, the asymmetry for antenna and brightness temperatures are very similar. The exact cause of the asymmetry remains unclear, how-

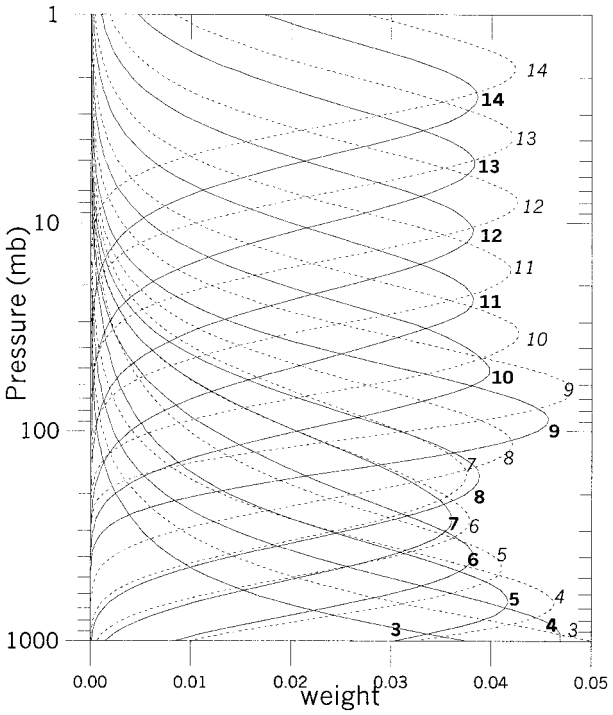

FIG. 3. AMSU-A channels 4–14 weighting functions for two view angles: near-nadir angle of 1.35 (solid curves) and the largest angle of 47.85 (dashed curves).

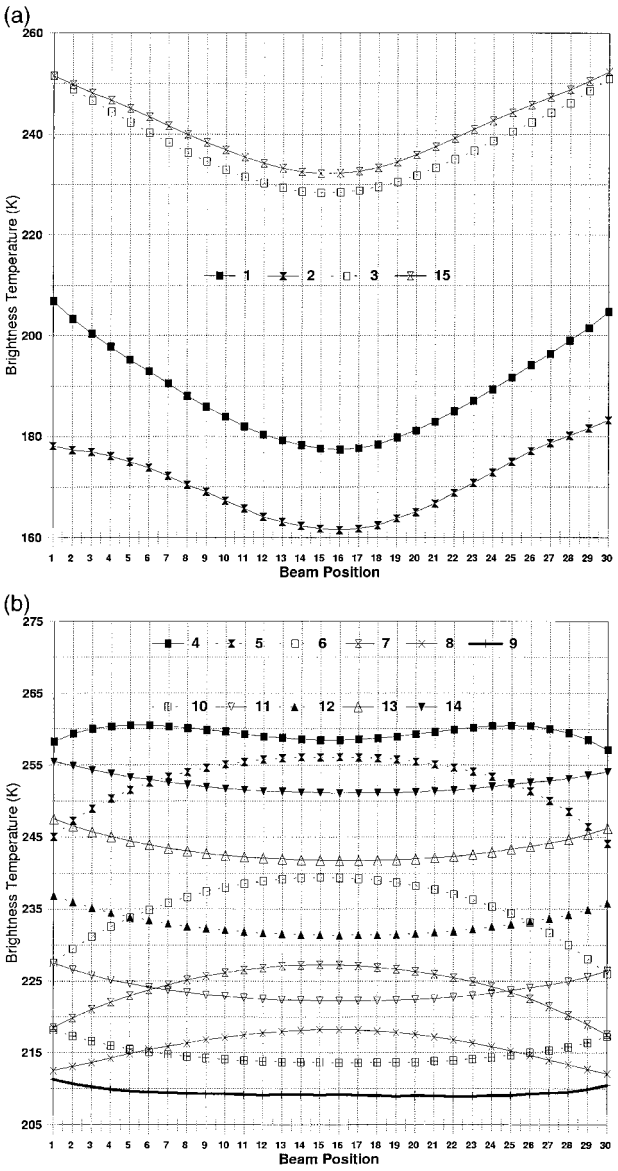

FIG. 4. Mean unadjusted brightness temperatures as a function of beam position [(a)—window channels, (b)—atmospheric channels].

ever, nearly all of the asymmetry is removed by the limb adjustment procedure.

The limb effect is caused by the increase in optical path as the instrument scans from near nadir to larger angles, which causes the peak of the channel weighting functions to increase in altitude. The weighting functions, which give the vertical contribution of atmospheric temperature to the outgoing radiance measured by the instrument, are shown for AMSU-A channels 3–14 at its near-nadir angle of 1.67° and the extreme angle of 48.33° (dashed curves) in Fig. 3. Mean variations of unadjusted brightness temperatures as a function of FOV are shown in Fig. 4. Differences between each position and the average of positions 15 and 16 (there is no true nadir position) for each channel are given in Fig. 5, and can be quite large. The deviations from the average of the two near-nadir values are not simple offsets, if they were, the standard deviations of the data, shown in Fig. 6, would be uniform with respect to FOV position. The standard deviations are not constant, at least in part because the atmospheric region contributing to the observations is a function of FOV.

Over the ocean, brightness temperatures for a given window channel increase with increasing view angle, because the channel is seeing less of the surface due to the increase in the optical path. Surface emissivity at these microwave frequencies is quite low, approximately 0.45 for channels 1 (23.8 GHz) and 2 (31.4 GHz), over the ocean, which result in very low brightness temperatures (less than 160 K for both channels 1 and 2 in clear and dry conditions). Even though the surface emissivity is increasing slightly away from nadir due to the polarization of the AMSU channels, the contribution from the atmosphere sharply increases the brightness temperature value with increasing view angle. Over land, because the emissivity is closer to unity, the mean variation in the window channel measurements, as a function of FOV, is very small (not shown). Limb cooling arises in channels peaking in the troposphere because the temperature profile generally decreases with height. In the stratosphere, the opposite occurs because the temperature is now generally increasing with height.

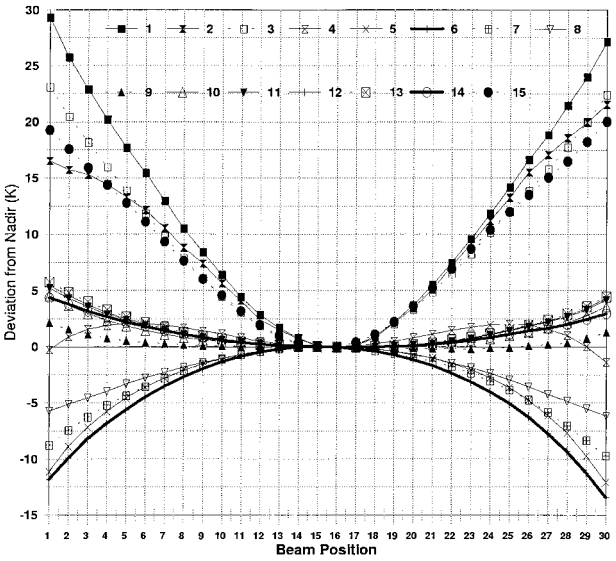

FIG. 5. The deviation of unadjusted brightness temperatures from nadir (average of positions 15 and 16) for all channels.

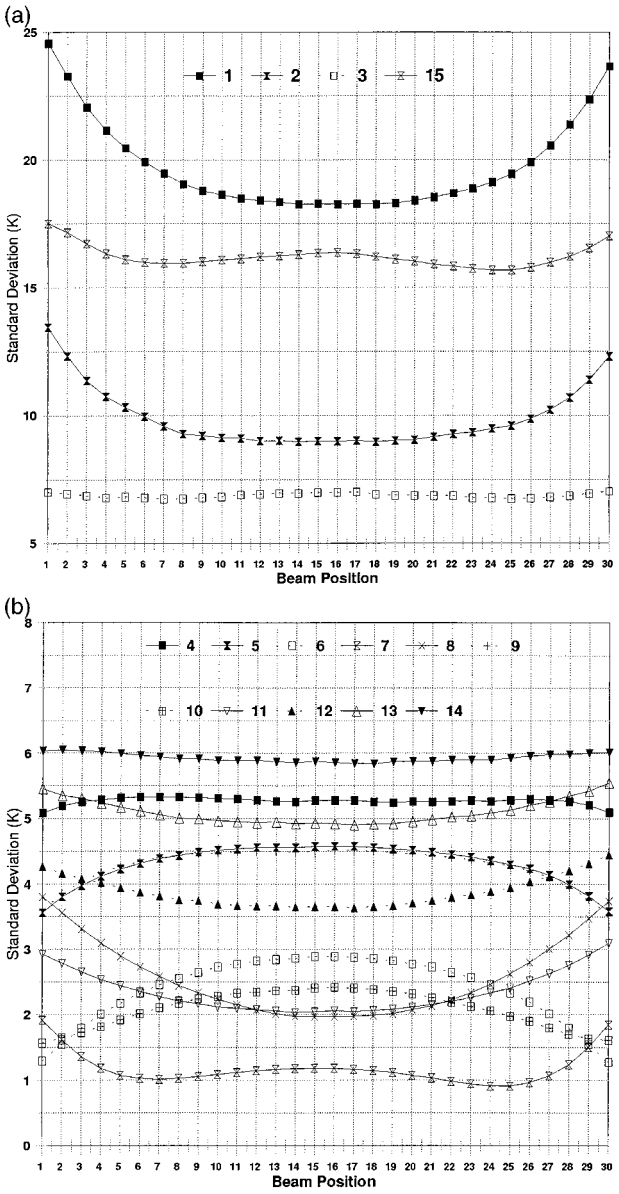

FIG. 6. The standard deviation of unadjusted brightness temperatures as a function of beam position [(a)—window channels, (b)—atmospheric channels].

Limb adjustment can be derived by either physical, statistical, or combinations of physical and statistical approaches. In a purely physical approach, one would solve for coefficients that combine weighting functions from the off-nadir position to best fit the nadir weighting functions. This procedure was carried using the technique described in Goldberg and Fleming (1995). Figure 7 shows the near-nadir weighting functions and linear combinations of extreme off-nadir weighting functions that approximate them. Clearly the AMSU-A data can be limb adjusted since the respective weighting functions in Fig. 7 are quite close in value. However, because of the asymmetry shown in Fig. 2, we cannot use a purely physical approach.

We first experimented with a purely statistical approach, similar to one first suggested by Wark (1993) and currently used operationally for AMSU-A and MSU. However, we found that for a few channels the coefficients from the statistical method were quite different from coefficients derived from a physical method. An example will be shown at the end of this section. Our solution to this observation is to use the physical coefficients as a constraint in the statistical model. The technique is a constrained least squares procedure and is similar to those in Goldberg and Fleming (1995) or Crone et al. (1996). The limb adjusted brightness temperature y is given by

$$y = \mathbf{x}^{\mathrm{T}}\mathbf{b}, \tag{1}$$

where $\mathbf{x}$ is a vector of unadjusted brightness temperatures and $\mathbf{b}$ is a vector of coefficients. To solve for $\mathbf{b}$, we use a training ensemble of observed y and $\mathbf{x}$. The ensemble does not include individual cases of y and $\mathbf{x}$, rather y and $\mathbf{x}$ are means over latitude bands from a large time period so that variations as a function of beam position are not due to variations in airmass and surface features. All the values below are deviations from a global mean. Let y_i be the mean of the average of positions 15 and l6 in a particular channel for latitude band, i. Let $\mathbf{x}_i = (x_{1i}, \ldots, x_{ki})^{\mathrm{T}}$ be a vector where $x_{1i}, \ldots, x_{ki}$ are the mean values over this latitude band and beam position of the channels that are to be used to estimate y. The subscript k refers to the number of channels used in a particular regression. Let $\mathbf{b}$ be the vector of coefficients to be estimated and let $\mathbf{b}_p$ be the set of physical coefficients derived using the technique described above.

In order to estimate $\mathbf{b}$ we define a penalty function

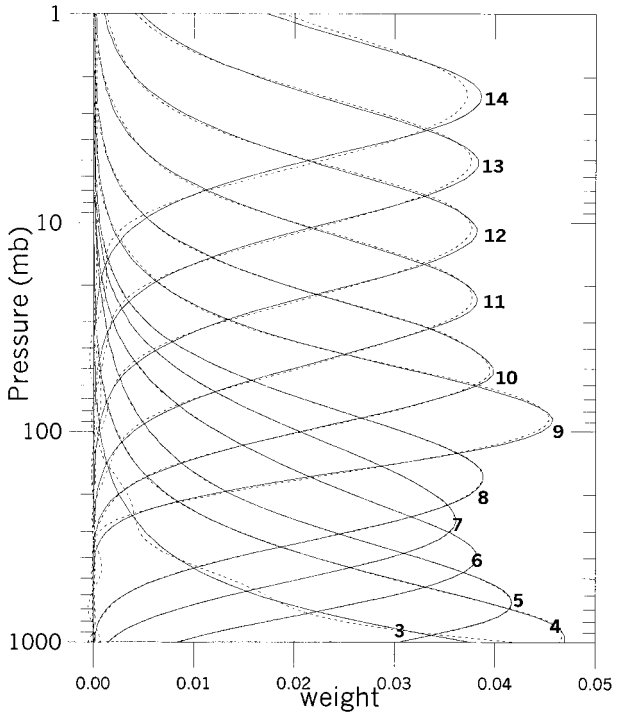

FIG. 7. AMSU-A channels 4–14 weighting functions for near-nadir (solid curves) and physically estimated (dashed curves) weighting functions from the largest off-nadir angle.

$$F(\mathbf{b}) = (\mathbf{X}^{\mathrm{T}}\mathbf{b} - \mathbf{y})^{\mathrm{T}}(\mathbf{X}^{\mathrm{T}}\mathbf{b} - \mathbf{y}) + \gamma(\mathbf{b} - \mathbf{b}_p)^{\mathrm{T}}(\mathbf{b} - \mathbf{b}_p) + 2\lambda(1 - \mathbf{u}^{\mathrm{T}}\mathbf{b}), \quad (2)$$

where γ and λ are Lagrange multipliers. In Eq. (2) $\mathbf{X}$ is a matrix of the $\mathbf{x}_i$s, $\mathbf{y}$ is a vector of means for all latitude bands, and $\mathbf{u}$ is a vector of ones. The first term of Eq. (2) represents the least squares fit to the measured data, the second term minimizes the deviation of the coefficients from the physically derived coefficients, and the third term requires that the coefficients sum to unity.

To minimize F with respect to **b,** we take the derivative and equate the result to the zero vector. This yields

$$2\mathbf{X}(\mathbf{X}^{\mathrm{T}}\mathbf{b} - \mathbf{y}) + 2\gamma(\mathbf{b} - \mathbf{b}_p) - 2\lambda\mathbf{u} = 0. \quad (3)$$

From Eq. (3) it follows that

$$\mathbf{b} = (\mathbf{X}\mathbf{X}^{\mathrm{T}} + \gamma\mathbf{I})^{-1}(\mathbf{X}_{\mathrm{y}} - \gamma\mathbf{b}_p - \lambda\mathbf{u}). \quad (4)$$

Then, using the condition that $\mathbf{u}^{\mathrm{T}}\mathbf{b} = 1$, we can solve for λ.

$$\lambda = \frac{1 - (\mathbf{X}\mathbf{X}^{\mathrm{T}} + \gamma\mathbf{I})^{-1}(\mathbf{X}\mathbf{y} - \gamma\mathbf{b}_p)}{\mathbf{u}^{\mathrm{T}}(\mathbf{X}\mathbf{X}^{\mathrm{T}} + \gamma\mathbf{I})^{-1}\mathbf{u}}. \quad (5)$$

This result is then substituted into Eq. (4) to solve for **b.** This leaves γ as the only unknown. The final results are obtained by tuning on γ. Because OPTRAN does not include the effects of cloud liquid water, the parameter γ was set to zero for the window channels.

Thirty-one days of data from 1 to 31 July 1998 were used to compute mean brightness temperatures within 2° latitude bands for each FOV. As mentioned above, means are used to assure that differences in brightness temperatures between two given FOVs are due to view angle and not due to atmospheric and surface variability. Using the above mean values, the physically constrained regression coefficients are then computed to adjust measurements from a given FOV to ''look like'' the average of beam positions 15 and 16 (there is no true nadir observation). That is, the mean brightness temperatures at the angle are the predictor or independent variables and the average of the mean brightness temperature of positions 15 and 16 is used as the response or dependent variable. A global set of coefficients is used for channels 6–14. Separate sea and nonsea coefficients are used for channels affected by the surface—channels 1–5 and 15. The predictors are generally the channel itself plus the adjacent channel whose weighting functions peak below and above. In other words to limb adjust channel 6, we use unadjusted channels 5, 6, and 7 observations as predictors. The exceptions are channel 14 uses channels 12, 13, and 14; channel 3 uses channels 3, 4, and 5; channel 1 and 2 both use channels 1 and 2, and channel 15 uses channels 1 and 15. Since the regression is carried out on mean values the usual measures such as R^2 (coefficient of determination) or s_e (root-mean-squared error) do not have their standard meaning. This model assumes that the limb effect can be adjusted using linear combinations of the channels at a given angle. The largest limb adjustment model error, usually associated with the furthest off-nadir positions, are given in Fig. 8. Also shown for comparison are the instrumental noise and a parameter we call combined atmospheric and instrument noise. This parameter is the root-mean-square (rms) difference between the same FOV position of adjacent scanlines within the tropical region where the temperature variability is assumed negligible. To get an unbiased estimate of the noise in a single FOV, the rms was divided by the square root of 2. The sample size for computing this parameter was approximately 10 000 for each FOV. For the temperature sounding channels the atmospheric/instrumental noise is nearly identical to the instrument noise. For the window channels the atmospheric/instrumental noise is much larger due to variability of water vapor and cloud liquid water. For all channels the limb adjustment model errors are lower than the atmospheric/instrumental noise. The larger model errors associated with the window channels are small relative to the observed range of these channels, which can be inferred from the standard deviations given in Fig. 6.

An example of the benefit of deriving physically constrained coefficients is shown in Fig. 9. Here the coefficients for limb adjusting channel 5 are plotted as a function of beam position. There are two sets: coefficients derived from the purely statistical approach and coefficients derived from the combine statistical/physical method. To limb adjust channel 5, channels 4, 5, and 6 are used as predictors. As shown in this figure, the statistical coefficient for the channel 5 predictor is

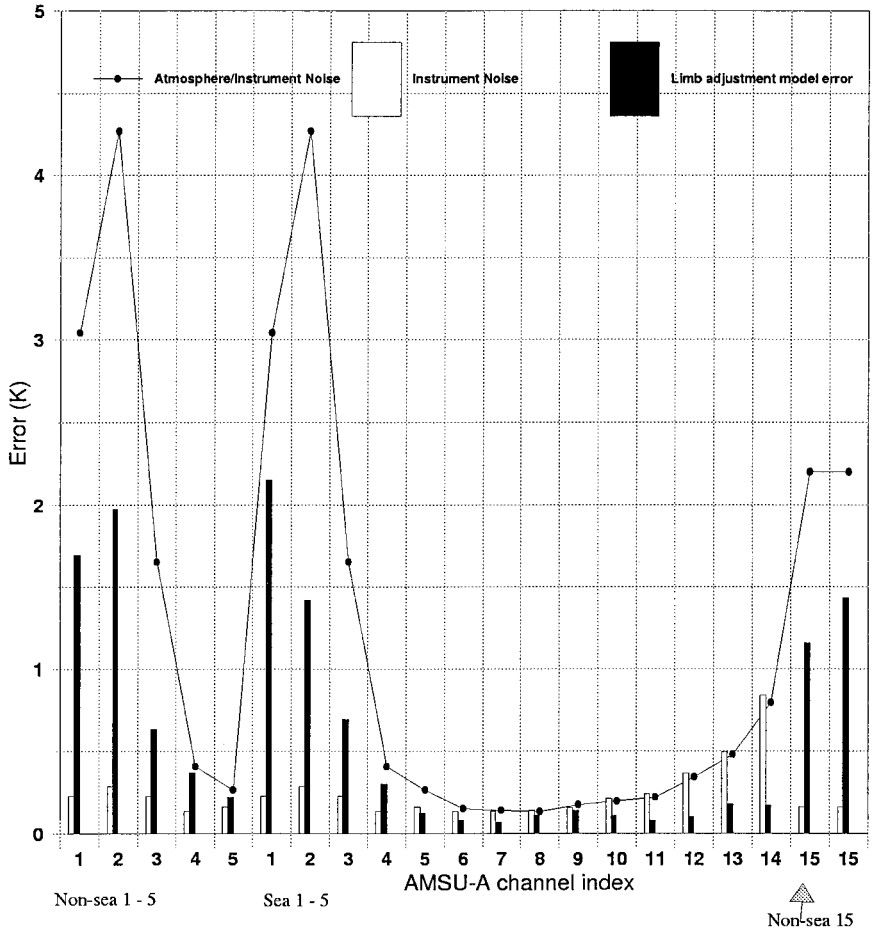

FIG. 8. The limb adjustment model error for each channel, along with instrumental noise and a composite noise consisting of instrument and atmospheric noise.

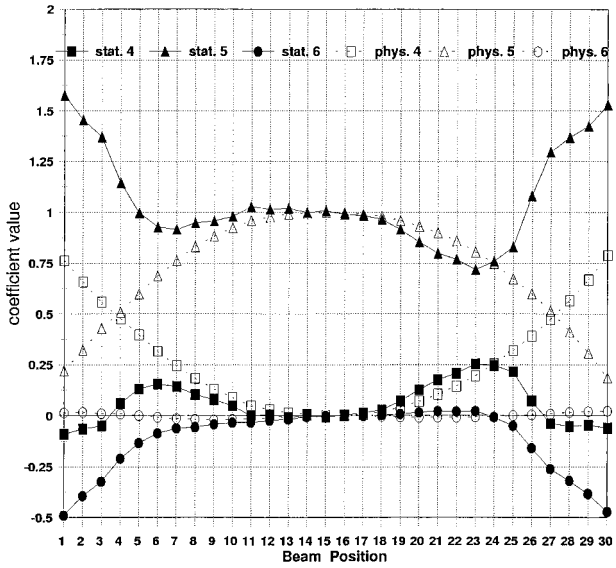

FIG. 9. Channel 5 limb adjustment coefficients for statistical approach (solid curves) and physically constrained approach (dashed).

much larger than the channel 4 predictor for beam position 1 (the largest off-nadir angle); however, as implied from Fig. 3, the coefficient for channel 4 should dominate, since the channel 4 weighting function at beam position 1 is similar to the channel 5 near-nadir weighting function. Note that the coefficients from the physical/statistical approach are all less than or equal to unity, which results in reduction of measurement noise; whereas the statistical approach allows coefficients much greater than unity, which result in a noise amplification of nearly 2.5 at the extreme angles. Amplification is determined by simply computing the square root of the sum of the square of the coefficients (in this example we assumed that each channel had equivalent measurement noise).

3. Validation

The limb adjustment procedure was validated in a number of ways. The simplest approach is to display fields of limb adjusted and unadjusted AMSU brightness temperatures as given in Fig. 10 for AMSU channel 5.

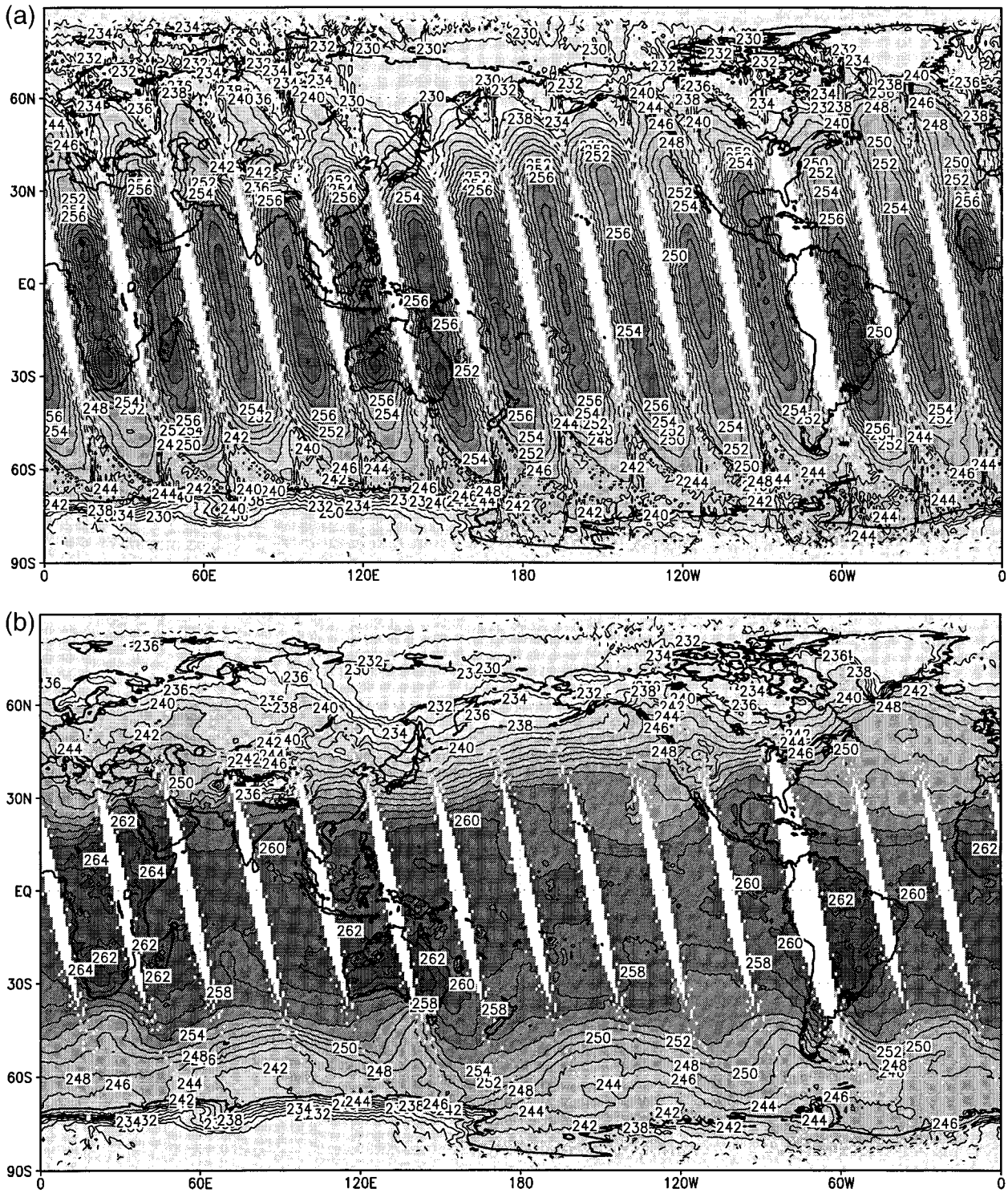

FIG. 10. (a) Global fields of unadjusted brightness temperatures and (b) limb adjusted brightness temperatures for channel 5.

This channel is representative of a lower-tropospheric deep-layer mean temperature near nadir, but becomes a midtropospheric deep-layer mean temperature at the extreme view angles. It is only when the observations are limb adjusted that interesting meteorological structures can been seen. For instance, the large temperature gradient associated with the jet stream over the northern Pacific Ocean. Visually, the limb adjustment appears to

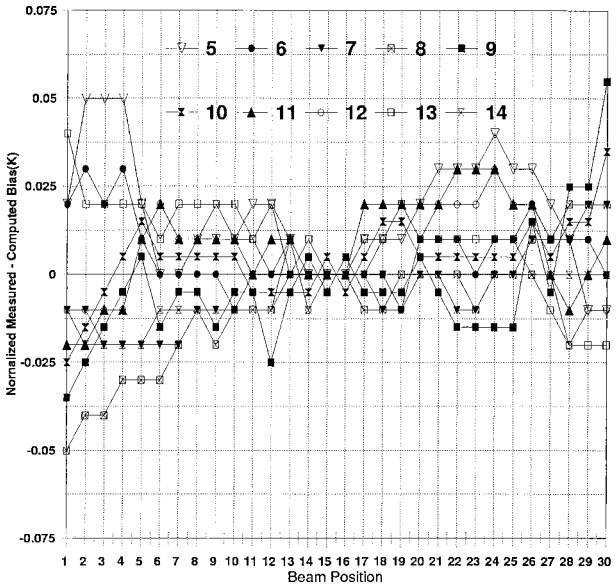

FIG. 11. Mean bias between limb adjusted brightness temperatures and brightness temperatures calculated from the NCEP 0000 UTC analysis of 2 May 1999.

work quite well for channel 5. Other examples can be found at our Internet site (http://orbit-net.nesdis.noaa.gov/crad/st/amsuclimate/amsu.html).

A more objective and rigorous validation involves comparing measured limb adjusted brightness temperatures and brightness temperatures computed using a radiative transfer model. The limb adjustment procedure is applied to all observations, however, the validation

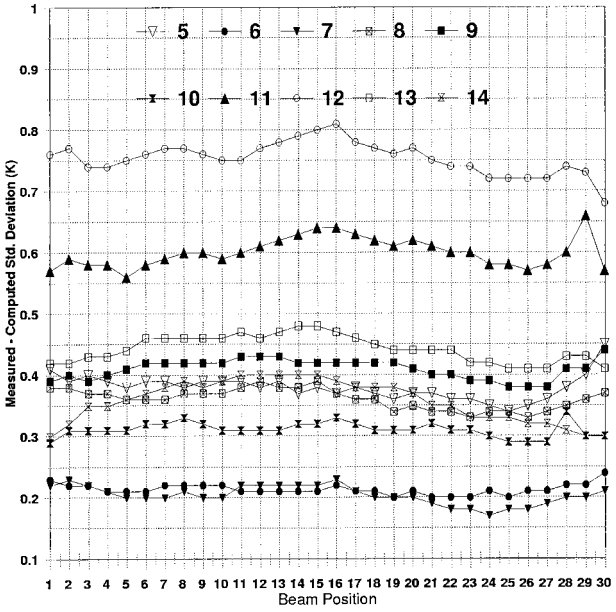

FIG. 12. Standard deviation between limb adjusted brightness temperatures and brightness temperatures calculated from the NCEP 0000 UTC analysis of 2 May 1999.

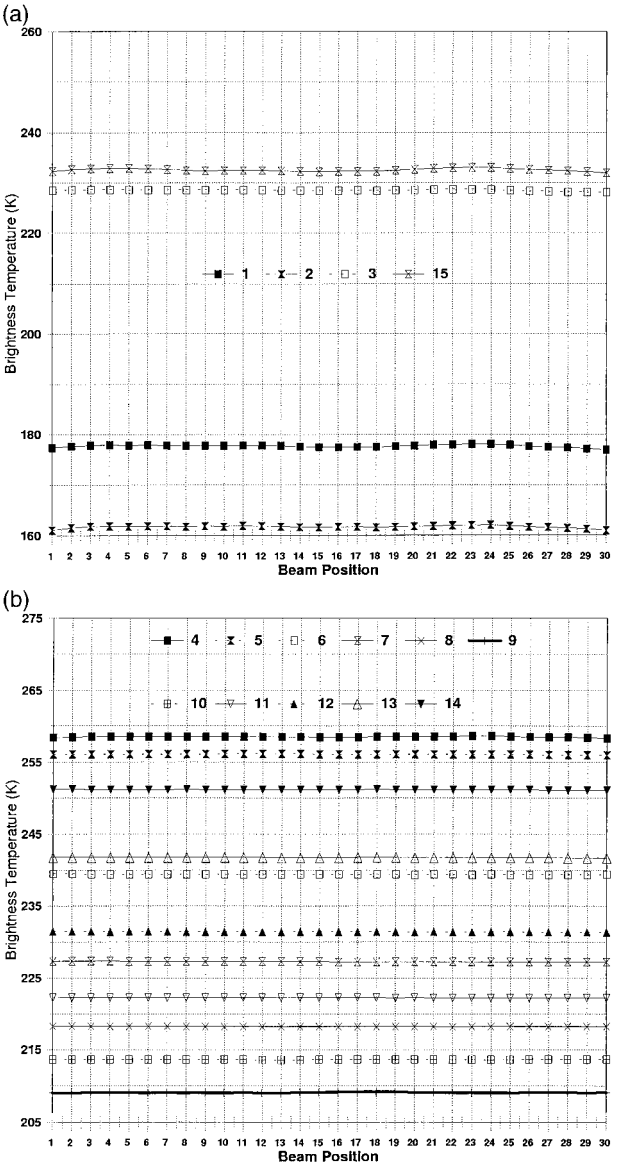

FIG. 13. Mean limb adjusted brightness temperatures as a function of beam position [(a)—window channels, (b)—atmospheric channels].

is limited to ocean-only observations because of the much larger variability and uncertainty of both surface emissivity and surface temperature over land. Note, however, that the ocean-only validation is representative for channels that are insensitive to the surface (channels 6–14). In this work we used OPTRAN (McMillin et al. 1995) to simulate AMSU-A nadir values. A comparison was made with collocated NCEP analysis reports. The analysis avoids the problem of nonuniform sample size, which would be present in radiosonde collocations. AMSU brightness temperatures were computed from the NCEP analysis for 2 May 1999. Figure 11 shows the bias between the limb adjusted and computed values for channels 5–14. The average of FOV positions 15 and

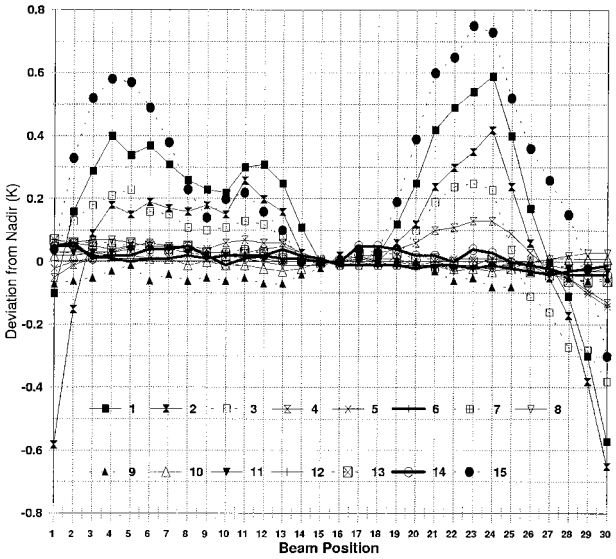

FIG. 14. The deviation of limb adjusted brightness temperatures from nadir (average of positions 15 and 16) for all channels.

16 were used to remove systematic differences between measured and computed values, which results in a near-zero bias for the near-nadir positions. The remaining channels are not computed because they are significantly influenced by cloud liquid water effects. Cloud liquid water from the analysis is prone to misrepresentation and furthermore OPTRAN does not include cloud liquid water attenuation in its computation. The average standard error between limb adjusted brightness temperatures and analysis nadir computed values as a function of FOV is shown in Fig. 12. The standard deviation for channel 5 is higher than channel 6 because of greater influence from the surface. Above channel 9, the reduction in the standard deviation is an artifact due to adding an AMSU-A temperature retrieval (Goldberg 1999) above the highest model pressure level of 10 mb. The variability of the standard deviation with respect to FOV is quite small.

To validate the window channels and channel 4, we produced figures comparable to Figs. 2, 4, 5, and 6, however, instead of unadjusted observations, the data shown is for limb adjusted brightness temperatures. The correspondence is as follows: Figs. 13, 14, 16, and 17

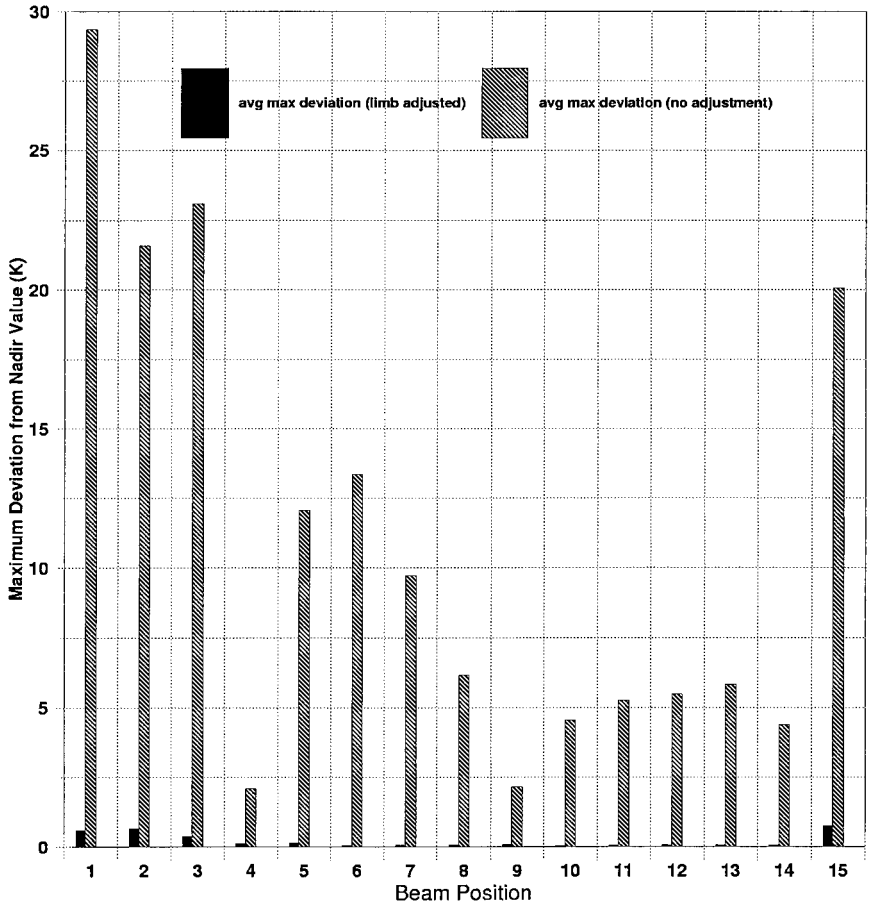

FIG. 15. The maximum deviation from nadir of limb adjusted and unadjusted brightness temperatures.

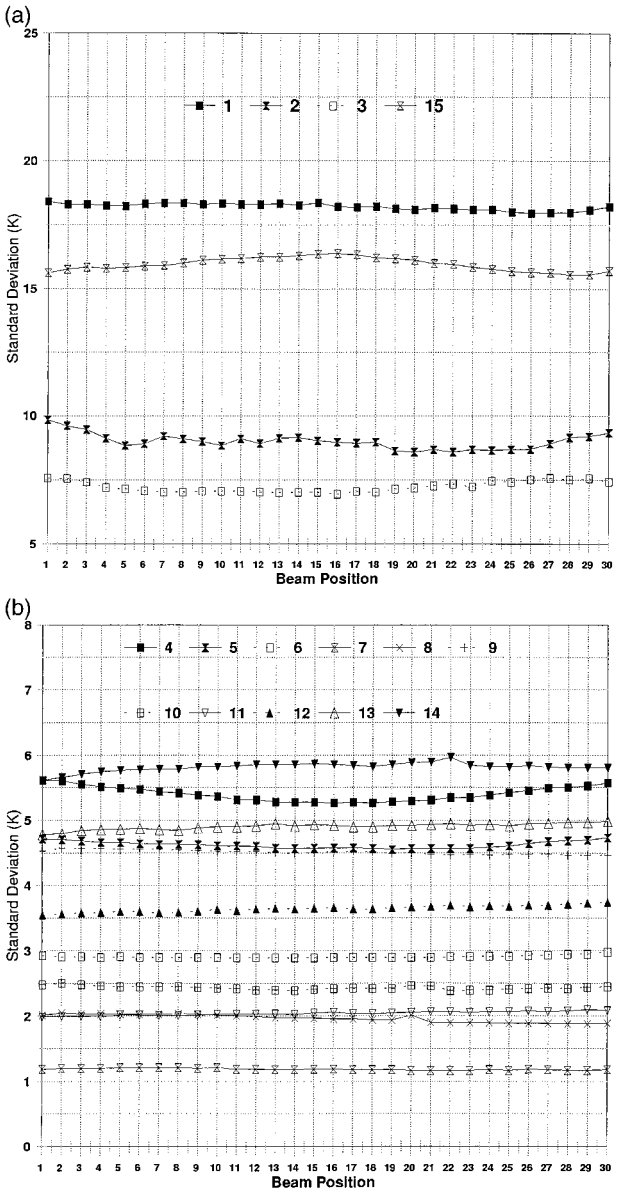

FIG. 16. The standard deviation of limb adjusted brightness temperatures as a function of beam position [(a)—window channels, (b)—atmospheric channels].

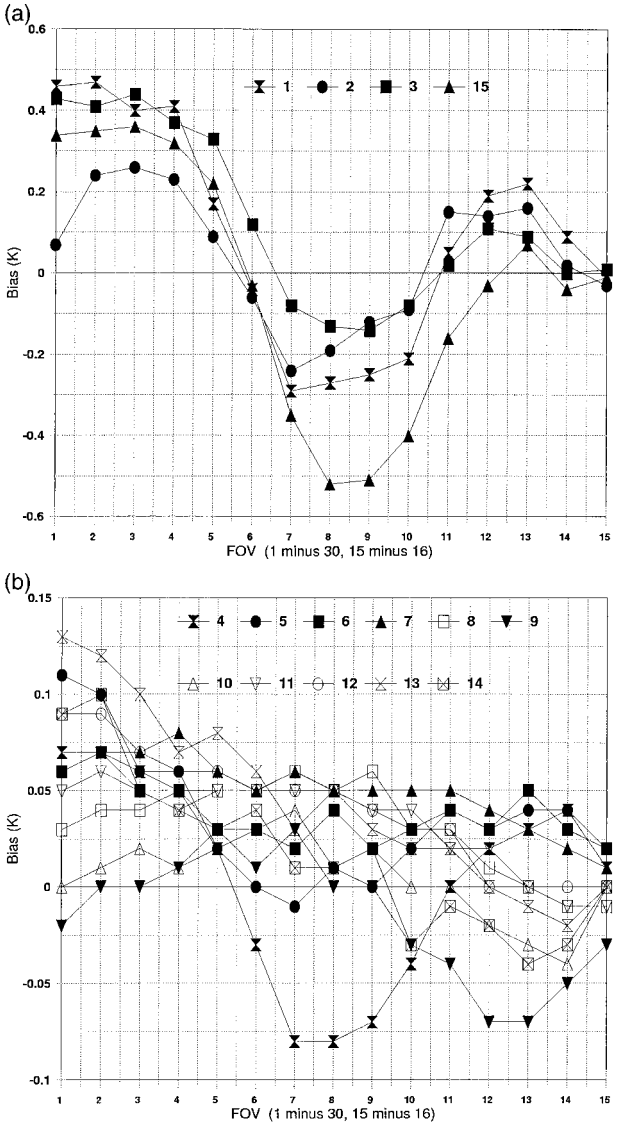

FIG. 17. The mean bias (i.e., asymmetry) between limb adjusted brightness temperatures from field-of-views with the same off-nadir angles: (a) the bias from the window channels, (b) the bias from the atmospheric channels.

are analogous to Figs. 4, 5, 6, and 2, respectively. Figure 13 show that the mean brightness temperatures are almost invariant with respect to FOV position. Each FOV mean value has a sample size of about 20 000, which should remove nearly all influence of atmospheric variability. Differences between each position and the average of positions 15 and 16 for each channel are given in Fig. 14, and clearly are quite small when compared with the unadjusted data in Fig. 5. The window channels have systematic biases that are as large as 0.8 K, but typically the average bias for those channels is about 0.2 K. Figure 15 shows a comparison of the largest deviation from nadir (average of positions 15 and 16) of unadjusted and limb adjusted data. Again, we observe that even though the bias in the limb adjusted window channels is much larger than that in the atmospheric temperature channels, the bias is much smaller than the unadjusted deviation. The standard deviation of limb adjusted brightness temperatures are given in Fig. 16. The standard deviations are quite uniform especially for the atmospheric channels. The 31.4-GHz channel 2 is an exception at the large scan angles, which needs further study. Windows are simply more difficult to limb adjust due to influences of surface emissivity, surface roughness, cloud liquid water, and water vapor. On the other hand, the limb adjustment procedure is performing quite well, considering that we are using a linear model

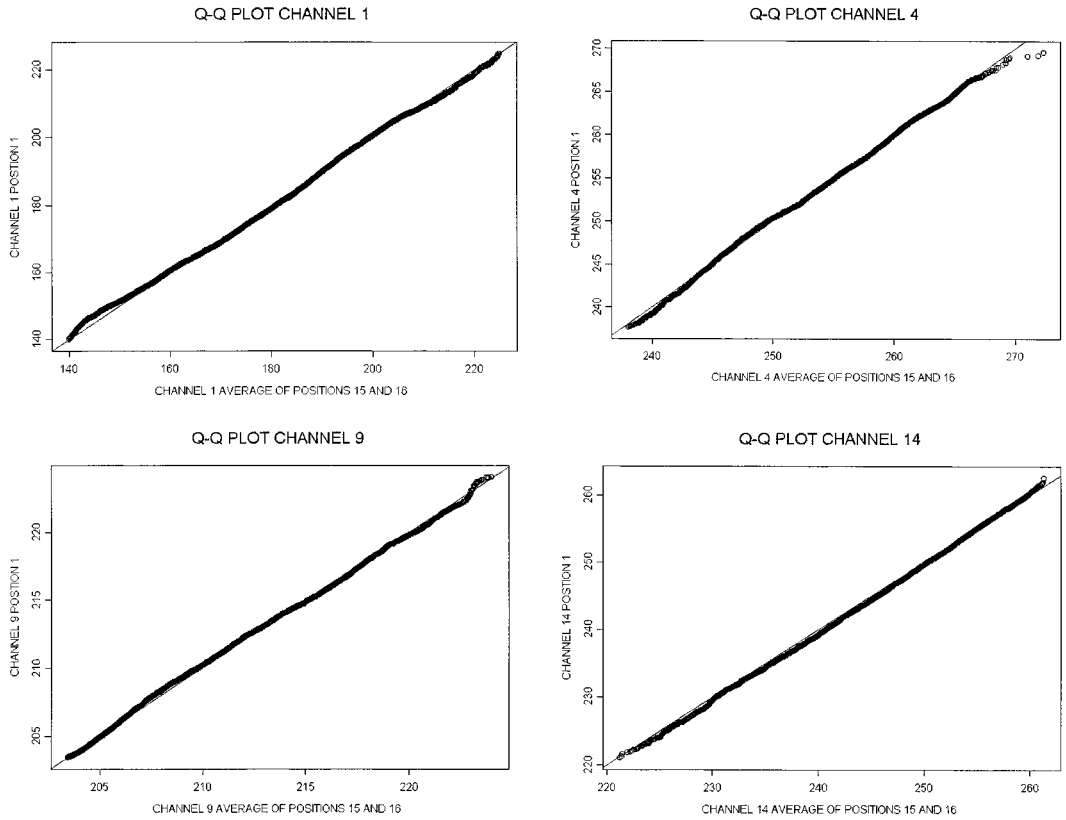

FIG. 18. Quantile–quantile plots for channels 1, 4, 9, and 14.

and that the coefficients were derived from data collected in July 1998 and are applied to May 1999 data. For completeness, the asymmetries of limb adjusted brightness temperatures are given in Fig. 17, and obviously is much smaller than the asymmetry of unadjusted brightness temperature shown in Fig. 2.

The basic assumption of the statistical evaluation techniques presented so far is that the distribution of the limb adjusted measurements should not be a function of scan angle. If the distributions are the same then the means and standard deviations will be the same. However, even if the mean and standard deviations are the same the distributions may be different. To further test the assumption that the distributions are the same we use quantile–quantile plots or q–q plots. The two sets of data are compared by graphing the quantiles of one distribution again the quantiles of the second distribution. If the two distributions are the same then this plot should be the line $x = y$, or the identity function over the range of values taken on by the two distributions. For a detailed discussion of q–q plots see Cleveland (1993). This graphical statistical technique gives an additional objective criterion for evaluating and comparing limb adjustment procedures. Figure 18 gives q–q plots for channels 1, 4, 9, and 14. These are a surface, lower, midlevel and upper-level peaking channels, respectively. It is seen from the q–q plots that the distributions are very close over nearly the entire range of possible values for these four channels. The results for the other channels are similar.

4. Application

The limb adjustment algorithm has been applied to AMSU-A data since July 1998. As mentioned in the introduction, our limb adjusted AMSU-A data has been used for studying the formation of tropical storms and by the authors to begin a data record of atmospheric temperature and moisture (see Internet site http://orbit-net.nesdis.noaa.gov/crad/st/amsuclimate/amsu.html).

The last validation experiment is to compare monthly means of limb adjusted atmospheric AMSU-A brightness temperatures near radiosonde locations with synthesized nadir AMSU-A values computed from collocated radiosonde reports of temperatures and moisture (see Fig. 19). The mean for each month is based on a sample size of about 120. The AMSU-A and radiosonde computed means are in very good agreement; the average standard deviation of the difference between the measured and computed means is about 0.09 K.

5. Summary

We have presented a method of limb adjusting AMSU-A observations. Our method is straightforward, and

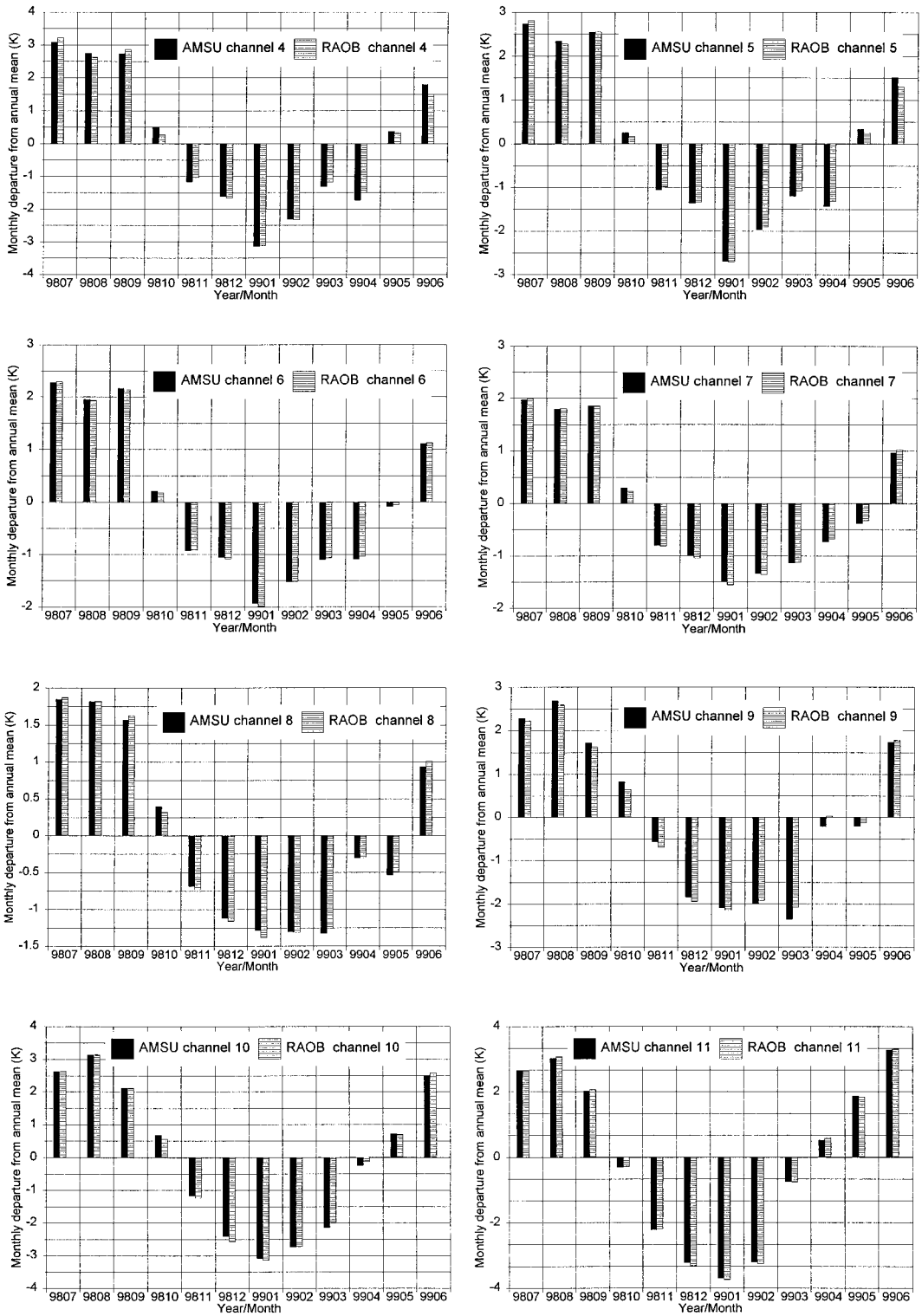

FIG. 19. Monthly departures from the annual mean for limb adjusted brightness temperatures and nadir brightness temperatures calculated from collocated radiosondes.

a rigorous validation has indicated that the adjustment of off-nadir observations to the average of the two nearest nadir positions (15 and 16) is excellent. We plan to use this method to establish a record of AMSU-A tropospheric and stratospheric temperatures to complement the record already established using data from the MSU (Spencer and Christy 1993) and the Stratospheric Sounding Unit (Nash and Forrestor 1986).

REFERENCES

Cleveland, W. S., 1993: *Visualizing Data.* Hobart Press, 360 pp.

Crone, L. J., L. M. McMillin, and D. S. Crosby, 1996: Constrained regression in satellite meteorology. *J. Appl. Meteor.,* **35,** 2023–2035.

Goldberg, M. D., 1999: Generation of retrieval products from AMSU-A: Methodology and validation. *Tech. Proc. 10th Int. TOVS Study Conf.,* Boulder, CO, Bureau of Meteorological Research Centre, 215–229.

——, and H. E. Fleming, 1995: An algorithm to generate deep-layer temperatures from microwave satellite observations for the purpose of monitoring climate change. *J. Climate,* **8,** 993–1004.

Grody, N. C., F. Weng, and R. Ferraro, 1999: Application of AMSU for obtaining water vapor, cloud liquid water, precipitation, snow cover, and sea ice concentration. *Tech. Proc. 10th Int. TOVS Study Conf.,* Boulder, CO, Bureau of Meteorological Research Centre, 230–239.

Hollinger, J. P., 1971: Passive microwave measurements of sea surface roughness. *IEEE Trans. Geosci. Electron.,* **GE-9,** 165–169.

Kidder, S. Q., M. D. Goldberg, R. M. Zehr, M. DeMaria, J. F. W. Purdom, C. S. Velden, N. C. Grody, and S. J. Kusselson, 2000: Satellite analysis of tropical cyclones using the Advanced Microwave Sounding Unit (AMSU). *Bull. Amer. Meteor. Soc.,* **81,** 1241–1259.

Klein, L. A., and C. T. Swift, 1977: An improved model for the dielectric constant of sea water at microwave frequencies. *IEEE Trans. Antennas Propag.,* **25,** 104–111.

McMillin, L. M., L. J. Crone, M. D. Goldberg, and T. J. Kleespies, 1995: Atmospheric transmittance of an absorbing gas: A computationally fast and accurate transmittance model for absorbing gases with fixed and with variable mixing ratios at variable viewing angles. 4. OPTRAN. *Appl. Opt.,* **34,** 6269–6274.

Mo, T., 1999: AMSU-A antenna pattern corrections. *IEEE Trans. Geosci. Remote Sens.,* **37,** 103–112.

Nash, J., and G. F. Forrestor, 1986: Long term monitoring of stratospheric temperature trends using radiance measurements obtained by the TIROS-N series of NOAA spacecraft. *Adv. Space Res.,* **6,** 37–44.

Smith, W. L., H. M. Woolf, C. M. Hayden, D. Q. Wark, and L. M. McMillin, 1979: The TIROS-N Operational Vertical Sounder. *Bull. Amer. Meteor. Soc.,* **60,** 1177–1187.

Spencer, R. W., and J. R. Christy, 1993: Precision lower stratospheric temperature monitoring with the MSU: Technique, validation, and results 1979–1991. *J. Climate,* **6,** 1194–1204.

Wark, D. Q., 1993: Adjustment of TIROS Operational Vertical Sounder data to a vertical view. NOAA Tech. Rep. NESDIS-64, 36 pp.